Vol. 44 (2013) ACTA PHYSICA POLONICA B No 7

STANDARD MODEL PHYSICS WITH τ LEPTONS IN THE FINAL STATE IN THE ATLAS EXPERIMENT*

Anna Kaczmarska†

on behalf of the ATLAS Collaboration

The H. Niewodniczański Institute of Nuclear Physics, Polish Academy of Sciences
Radzikowskiego 152, 31-342 Kraków, Poland

(Received April 17, 2013)

The ATLAS physics program involving τ final states ranges from Standard Model measurements involving W, Z, and top pair production, to searches for the Higgs boson, Supersymmetry and other signatures beyond the Standard Model. In this article, an overview is presented of the Standard Model studies done in ATLAS with τ leptons in final states: cross section measurements of W, Z and $t\bar{t}$ production and a τ polarization measurement in W decays.

DOI:10.5506/APhysPolB.44.1481
PACS numbers: 14.60.Fg, 13.35.Dx, 13.38.Be, 13.38.Dg

1. Introduction

τ leptons play an important role in the ATLAS physics program as they provide a useful signature in searches for the Standard Model Higgs boson and new phenomena in a wide range of theoretical models [1]. Measurements using Standard Model (SM) processes are a crucial step in the ATLAS physics program. τ leptons play an important role in such studies. Decays of SM gauge bosons to τ leptons, $W \to \tau\nu$ and $Z \to \tau\tau$, are important in the search for New Physics phenomena as they are dominant background processes in such searches. Thus, their production cross sections need to be measured precisely. Studies of $W \to \tau\nu$ and $Z \to \tau\tau$ processes at the LHC centre-of-mass energies are also interesting in their own right, complementing the measurements of the production of Z and W bosons in the electron and muon decay modes. Finally, these processes are essential for calibration of τ energy and for measurements related to τ lepton detection performance.

* Presented at the Cracow Epiphany Conference on the Physics After the First Phase of the LHC, Kraków, Poland, January 7–9, 2013.

† Supported, in part, by the Polish Government grant NN202 127937 (years 2009–2013).

At the LHC, top quark pairs ($t\bar{t}$) are produced in abundance due to the high centre-of-mass energy. In that case, one or both W bosons from top quark decays can decay further to τ leptons. This process is characterized by a higher number of jets in the event, coming from hadronic W boson decays and b-quarks and gives a different environment compared to $W \to \tau\nu$ and $Z \to \tau\tau$ processes. It leads also to a more complex and difficult reconstruction. This final state can provide an important alternative measurement of the top quark pair production cross section. It can be also further used as an input in searches of the possible charged Higgs production via top quark decays.

The τ lepton is the heaviest lepton. Its measured rest mass is 1776.82 ± 0.16 MeV [2]. The τ lepton is unstable, it has a mean lifetime of $(290.6 \pm 1.0) \times 10^{-15}$ s, corresponding to the proper lifetime of 87.11 μm [2]. The τ lepton is the only lepton heavy enough to decay leptonically and hadronically. In 35.2% of the cases, τ lepton decays leptonically and in 64.8%, into one or more hadrons [2]. Considering only hadronically decaying τ leptons, decays with only one charged particle (so-called *1-prong*) occur in about 72% of the cases and with three charged particles (so-called *3-prong*) in about 23%. The hadronic final states are dominated by $\pi^{\pm}$ and π^{0} mesons.

2. Reconstruction and identification of τ leptons

The reconstruction and identification of τ leptons at hadron colliders are challenging from the experimental point of view. Since purely leptonic τ decays are very difficult to distinguish from prompt electrons or muons, the τ identification algorithms are developed to efficiently reconstruct and identify the visible part (without the neutrino) of the hadronic decay modes, referred to here by $\tau_{\mathrm{had-vis}}$. The challenge, when identifying hadronic τ decays, is that their signatures in the detector are very similar to quark- or gluon-initiated jets from QCD processes. In addition, these background processes have cross sections many orders of magnitude greater than the cross sections for weak interaction processes involving τ leptons. The most discriminating features for identifying $\tau_{\mathrm{had-vis}}$ from this QCD multijet background are the τ leptons characteristic 1- or 3-prong signature and the relatively narrow clustering of tracks and energy deposits in the calorimeters. Electrons and muons can also be misidentified as 1-prong τ decays. Separate procedures have been developed for rejecting electrons and muons as their signatures are different from QCD jets [3].

The τ reconstruction algorithm relies on the inner detector and calorimeter information [4]. It starts from reconstructed jets by considering each of them as a $\tau_{\mathrm{had-vis}}$ candidate. The list of calorimeter clusters associated with $\tau_{\mathrm{had-vis}}$ candidate is then refined and used to calculate kinematic quantities. Tracks satisfying dedicated selection criteria are associated with the calorimeter clusters within a narrow cone. A list of identification variables is then calculated using information from tracking and calorimetry. The τ identification algorithm combines these variables into multivariate discriminants to reject fake candidates. Finally, selection on the output of the discriminants is used at the analysis level to select a sample of $\tau_{\mathrm{had-vis}}$ candidates with the desired level of background rejection and signal efficiency.

Two independent τ identification methods using boosted decision trees (BDT) and log-likelihood (LLH) algorithms are used to reject QCD jets [3]. τ lepton candidates are selected by requiring that the BDT or LLH output exceed a certain threshold, the value of which depends on the $\tau_{\mathrm{had-vis}}$ candidate transverse momentum, on the number of vertices reconstructed in the event and is chosen separately for 1-prong and multi-prong (with more than one track) $\tau_{\mathrm{had-vis}}$ candidates. The cut-based or BDT algorithms are used to reject muons and electrons faking $\tau_{\mathrm{had-vis}}$ candidates.

The example of performance of the $\tau_{\mathrm{had-vis}}$ identification methods for 1-prong $\tau_{\mathrm{had-vis}}$ candidates is illustrated in figure 1, in which the inverse background efficiencies for QCD jets (left) and electrons (right) faking $\tau_{\mathrm{had-vis}}$ candidates are shown as a function of the $\tau_{\mathrm{had-vis}}$ identification efficiency.

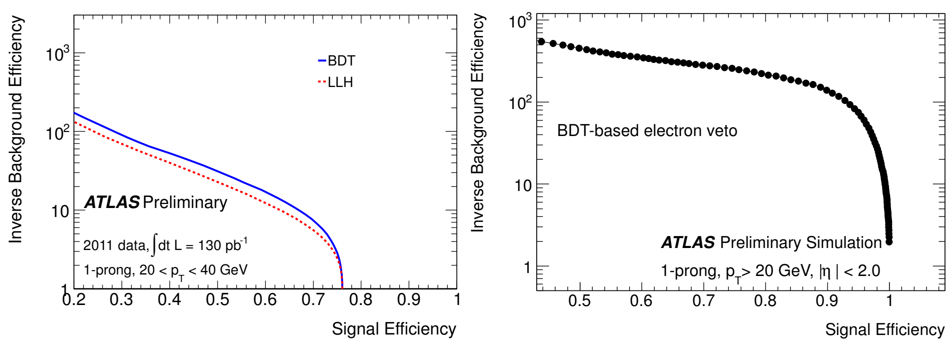

Fig. 1. (Left) Inverse background (QCD jets) efficiency *versus* signal efficiency for the BDT and LLH discriminants on 1-prong $\tau_{\mathrm{had-vis}}$ candidates in the low p_{T} range, 20 GeV $< p_{\mathrm{T}} \leq$ 40 GeV. (Right) Inverse background (electron) efficiency as a function of signal efficiency for 1-prong $\tau_{\mathrm{had-vis}}$ candidates with $p_{\mathrm{T}} >$ 20 GeV, in the central ($|\eta| < 2.0$) region, for the electron BDT discriminant [3].

3. $Z \to \tau\tau$ cross section measurement

The $Z \to \tau\tau$ cross section is measured in three different final states determined by the decay modes of the τ leptons [5]. The analysis is based on 1.34–1.55 fb^{-1} of $\sqrt{s} = 7$ TeV proton–proton collision data, depending on the final state. Three final states considered are: $Z \to \tau\tau \to \mu$+hadrons+3ν (denoted as $\tau_\mu\tau_h$), $Z \to \tau\tau \to e + \text{hadrons} + 3\nu$ (denoted as $\tau_e\tau_h$) and $Z \to \tau\tau \to e\mu + 4\nu$ (denoted as $\tau_e\tau_\mu$) with branching fractions $(22.50 \pm 0.09)\%$, $(23.13 \pm 0.09)\%$ and $(6.20 \pm 0.02)\%$, respectively.

The QCD multijet production is the dominant background for the $\tau_\mu\tau_h$ and $\tau_e\tau_h$ final states. A QCD jet can fake an electron, or have a real electron or muon from semileptonic decay of heavy quark or fake a hadronic τ decay. However, the reconstructed leptons from multijets, fake or real, often have other jet particles in their immediate neighbourhood. Leptons from signal events are usually isolated. Another background consists of events where a W boson decays to a light lepton, and is accompanied by a jet which fakes a hadronic τ decay. Muons and electrons in $Z \to ee/\mu\mu$ events can also occasionally fake hadronic τ decays as well. $t\bar{t}$ events are complex, and they feature various jets and leptons. They are easier to eliminate due to the larger number of objects and larger transverse momentum in the event, but incompletely reconstructed $t\bar{t}$ events can still fake the signal.

The following event selection is applied to suppress the various backgrounds. The muon trigger with an isolation requirement is used in the $\tau_\mu\tau_h$ and $\tau_e\tau_\mu$ final states, while a combined electron and hadronic τ trigger is used in the $\tau_e\tau_h$ final state. Next, exactly one muon candidate (or electron) and a hadronic τ is required in the $\tau_\mu\tau_h$ ($\tau_e\tau_h$) final states. Similarly, one muon and one electron with opposite charges are searched in the $\tau_e\tau_\mu$ final state. The isolation criteria are required for electrons and muons in order to reject QCD multijet background.

Special cuts reducing the W+jets background are applied, based on different event topology in signal and W+jets events. The $t\bar{t}$ background contributes significantly in the $\tau_e\tau_\mu$ channel. Contrary to $Z \to \tau\tau$, $t\bar{t}$ events are characterized by multiple high-p_{T} jets and leptons and large missing transverse energy, $E_{\mathrm{T}}^{\mathrm{miss}}$ [1]. Thus a selection is made by requiring that events have sum of E_{T} of all reconstructed objects and $E_{\mathrm{T}}^{\mathrm{miss}} < 140$ GeV. Finally, the $Z \to ee/\mu\mu$ background is reduced by requiring the invariant mass of the visible parts of the decay (*i.e.* not considering the neutrinos) to be within the mass window 35 GeV to 75 GeV. The visible mass distributions for all three channels are shown in figure 2.

[1] The missing transverse energy, $E_{\mathrm{T}}^{\mathrm{miss}}$, is defined as the momentum imbalance in the plane transverse to the beam axis.

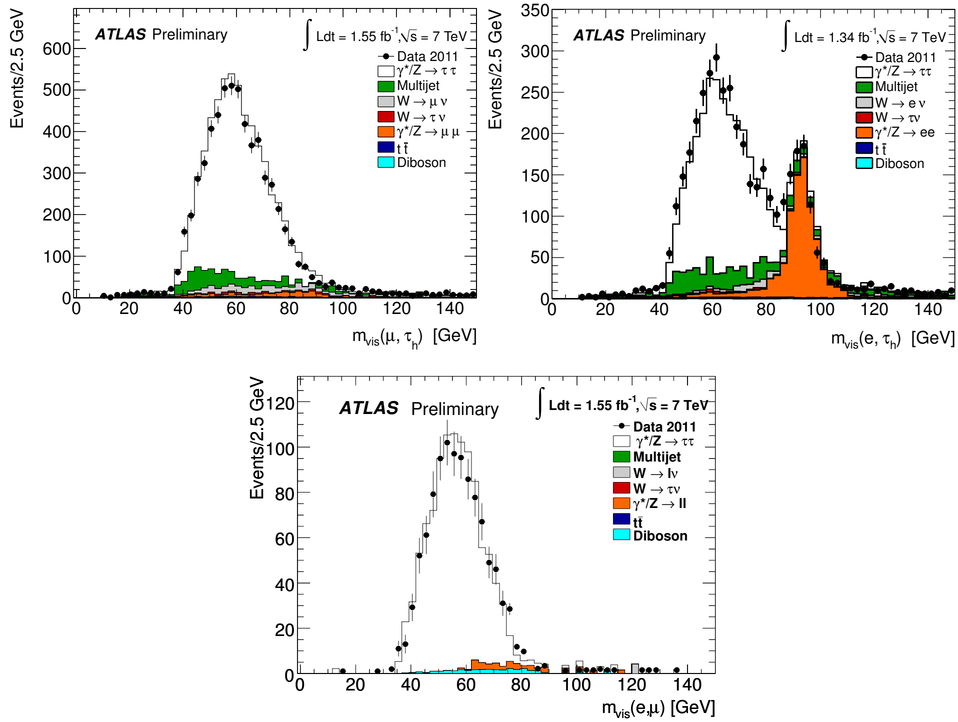

Fig. 2. The distributions of the visible mass after all selection cuts, except that on the visible mass, in the $\tau_\mu\tau_h$ (top left) and $\tau_e\tau_h$ (top right) and $\tau_e\tau_\mu$ (bottom) final states [5].

Contributions of the non-dominant backgrounds ($t\bar{t}$ and dibosons in all three final states and W, Z in the $\tau_e\tau_\mu$ final state) are obtained from Monte Carlo simulations. All other backgrounds (QCD multijet in all three final states and W, Z backgrounds in $\tau_\mu\tau_h$ and $\tau_e\tau_h$ final states) are derived by partially or fully data-driven methods. Normalization factors are derived in W/Z-enriched control regions to correctly scale the Monte Carlo predictions. The QCD multijet background contribution is estimated from the multijet-enriched region with inverse isolation requirement on the lepton and is extrapolated to the signal region.

The resulting measured $Z \to \tau\tau$ cross section is obtained by subtracting the estimated number of background events from the number of observed events in the signal region, and then taking into account factors for the geometrical acceptance of the detector and the kinematic region probed by the analysis, the efficiency of the event selection, and the luminosity. Several sources of systematic effects have been studied. The dominant systematic uncertainties contributing in all three final states are the energy scale, luminosity and acceptance uncertainty. For the $\tau_\mu\tau_h$ and $\tau_e\tau_h$ channels, the uncertainty on the τ identification efficiency is important, while the τ and electron trigger efficiencies are important for the $\tau_e\tau_h$ final state.

Cross sections are measured individually for each final state in a fiducial kinematic phase space, and also extrapolated to the full phase space in the invariant mass region 66–116 GeV. The separate cross sections are combined and the product of the total Z production cross section and $Z \to \tau\tau$ branching fraction is measured to be $0.92 \pm 0.02(\mathrm{stat}) \pm 0.08(\mathrm{syst}) \pm 0.03(\mathrm{lumi})$ nb, which is in agreement with the NNLO theoretical expectation [6] of 0.96 ± 0.05 nb.

The measured cross sections for the different $Z \to \tau\tau$ final states are shown in figure 3, as well as the combined $Z \to \tau\tau$ cross section.

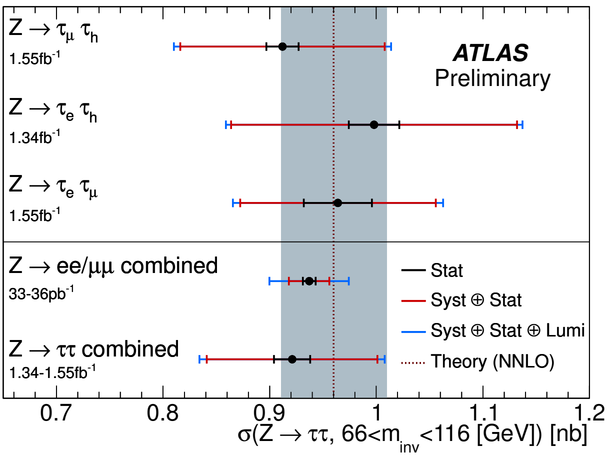

Fig. 3. The individual $Z \to \tau\tau$ cross section measurements by final state, and the combined result. The cross sections measured by ATLAS in the $Z \to \mu\mu$ and $Z \to ee$ final states is also shown for comparison [5]. The grey band indicates the uncertainty on the NNLO cross section prediction.

4. $W \to \tau\nu$ cross section measurement

The $W \to \tau\nu$ cross section measurement was performed using dataset corresponding to an integrated luminosity of 34 pb^{-1} at $\sqrt{s} = 7$ TeV [7]. Only final states, where the τ lepton decays hadronically are considered. The event signature is large $E_{\mathrm{T}}^{\mathrm{miss}}$ and one $\tau_{\mathrm{had-vis}}$ candidate containing either one or three tracks. Thus events are selected using combined triggers based on the presence of a $\tau_{\mathrm{had-vis}}$ candidate and $E_{\mathrm{T}}^{\mathrm{miss}}$. Events are further selected with offline cuts on p_{T} of $\tau_{\mathrm{had-vis}}$ candidate, $20 < p_{\mathrm{T}} < 60$ GeV, and $E_{\mathrm{T}}^{\mathrm{miss}} > 30$ GeV. $Z \to ee$, $Z \to \mu\mu$, $W \to e\nu$ and $W \to \mu\nu$ backgrounds are rejected by vetoing on the presence of an identified electron or muon, while the QCD multijet background is removed with a cut on the $E_{\mathrm{T}}^{\mathrm{miss}}$ significance, $S_{E_{\mathrm{T}}^{\mathrm{miss}}}$, ($S_{E_{\mathrm{T}}^{\mathrm{miss}}} > 6.0$) defined as

$$S_{E_{\mathrm{T}}^{\mathrm{miss}}} = \frac{E_{\mathrm{T}}^{\mathrm{miss}}[\mathrm{GeV}]}{0.5\sqrt{\mathrm{GeV}}\sqrt{(\sum E_{\mathrm{T}}[\mathrm{GeV}])}}\,. \tag{1}$$

The number of expected events from signal and electroweak background processes is obtained from simulation. An embedding technique is used as a cross-check of the results derived from MC. The muon in a high-purity sample of $W \to \mu\nu$ events is replaced by a simulated τ lepton. Thus, only the τ decay and the corresponding detector response are taken from simulation while the underlying W kinematics and all the other properties of the event are obtained from data. The QCD multijet background contribution is estimated from data in the multijet-enriched region with inverse τ identification and an inverted cut on the $E_{\mathrm{T}}^{\mathrm{miss}}$ significance.

In figure 4, the distribution of the number of tracks associated to the $\tau_{\mathrm{had-vis}}$ candidate, after full event selection, is shown. It illustrates the characteristic properties of $W \to \tau\nu$ events with a hadronic decay of τ lepton. The reasonable agreement is observed between the data and Monte Carlo prediction.

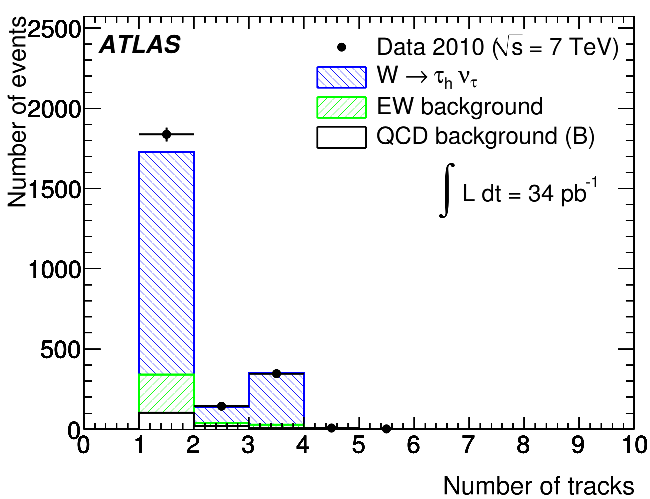

Fig. 4. Number of tracks of $\tau_{\mathrm{had-vis}}$ candidates after full event selection [7].

Several sources of systematic effects have been studied. The dominant systematic uncertainties are trigger and τ identification efficiencies and the τ energy scale.

The product of the total W production cross section and the $W \to \tau\nu$ branching ratio was measured to be $11.1 \pm 0.3(\mathrm{stat}) \pm 1.7(\mathrm{syst}) \pm 0.4(\mathrm{lumi})$ nb. The measured cross section is in a good agreement with the theoretical NNLO cross section and the ATLAS measurements of the $W \to e\nu$ and $W \to \mu\nu$ cross sections. The comparison of the cross section measurements for the different lepton final states and the theoretical expectation is shown in figure 5.

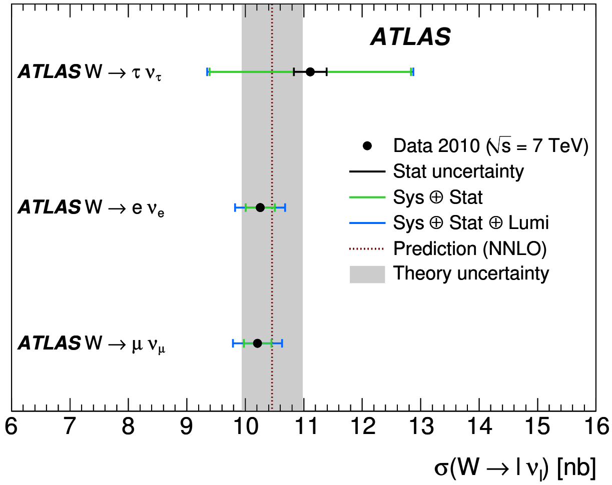

Fig. 5. Cross sections for the different $W \to$ lepton ν channels measured in ATLAS with 2010 data (points). Systematic, luminosity and statistical uncertainties are added in quadrature. The theoretical NNLO expectation is also shown (dashed line), together with its uncertainty (filled area) [7].

5. τ identification efficiency measurement

The performance and systematic uncertainties of the τ identification methods are evaluated on data using two different signal channels [3]. Three measurements are performed, two based on $Z \to \tau\tau$ and one based on $W \to \tau\nu$ events. These two processes have been chosen because they have specific signatures which can be selected by tag-and-probe methods. Also they make possible to get the sample of $\tau_{\mathrm{had-vis}}$ of a high purity without any τ identification requirement. All methods follow closely the W and Z cross section measurements, described in two previous sections.

In the $Z \to \tau\tau$ sample, one τ is considered to decay into a muon, which is used to select the event (a tag). The second τ lepton decays hadronically and is used to measure the τ identification efficiency (a probe). In the case of $W \to \tau\nu$, events the presence of large $E_{\mathrm{T}}^{\mathrm{miss}}$ is a tag and $\tau_{\mathrm{had-vis}}$ candidate is a probe. The identification efficiency is defined as the fraction of the probe

$\tau_{\rm had-vis}$ candidates that pass the τ identification. This efficiency is measured in data and estimated in Monte Carlo simulations using the same event selection. The ratio of these efficiencies is called the data/MC correction factor and is further used in all studies of processes with $\tau_{\rm had-vis}$ candidates from simulation in the final state.

The first τ efficiency measurement is based on $Z \to \tau\tau$ events and uses the method described in Section 3 for the QCD background estimation. The second one is also based on $Z \to \tau\tau$ events, but the background estimation is performed with a fit of the track multiplicity distribution of the probe $\tau_{\rm had-vis}$ candidate. The third measurement is based on $W \to \tau\nu$ events and also uses a fit of the track multiplicity of the probe $\tau_{\rm had-vis}$ for the background estimation. All of these measurements have many common features, but also significant differences, especially in the definition of the probe $\tau_{\rm had-vis}$ candidate. Thus a direct comparison of measured identification efficiencies is difficult. Nevertheless, the agreement or disagreement between what is measured in data and what is estimated in Monte Carlo simulations should be similar across all measurements. No significant deviation from unity has been observed in the correction factors in all three measurements. This means that the τ identification efficiency is well reproduced in simulations.

6. $t\bar{t}$ cross section measurement

The measurement of the $t\bar{t}$ production cross section in different decay channels is also an important test of the SM. Differential measurements of the $t\bar{t}$ production are especially important for testing and tuning the accuracy of different Monte Carlo generators, QCD models and parton distribution functions. On top of that, $t\bar{t}$ events are an important background in various Higgs and new physics searches, and it is, therefore, crucial to understand this process in detail.

New Physics can have influence on both the $t\bar{t}$ production and decay, modifying the observed $\sigma(t\bar{t})$ differently in different decay channels and/or affecting differential distributions. In particular, the cross section using final states including τ leptons is sensitive to New Physics phenomena such as the charged Higgs boson, predicted by the supersymmetric model. In the following, analyses in the τ + lepton channel ($t\bar{t} \to [b\tau_{\rm had-vis}][b\ e/\mu\ \nu]$) [8] and in the τ + jet channel ($t\bar{t} \to [b\tau_{\rm had-vis}][bqq]$) [9] are shortly described.

6.1. τ+jets final state

This measurement is based on 1.67 fb^{-1} of data, where one top quark decays into a τ lepton, a b-quark and a neutrino, and the other decays hadronically, resulting in a final state consisting of a hadronically decaying

τ lepton and jets. The data sample was selected with a b-jet trigger that required at least four jets, where two are identified as b-jets using a dedicated high-level trigger b-tagging algorithm.

Events are selected with at least five jets (two b-tagged) where one is selected as a $\tau_{\mathrm{had-vis}}$ candidate. The hadronic top quark is reconstructed using the combination of three jets, where one is b-tagged, that have the highest four-vector transverse momentum sum. The $\tau_{\mathrm{had-vis}}$ candidate is chosen from the remaining non-b-tagged jets that has the highest transverse momentum.

The characteristic track multiplicity of the $\tau_{\mathrm{had-vis}}$ candidate (n_{track}) distribution provides an excellent variable to separate the signal from background, which is dominated by QCD multijet events. To extract the signal from the n_{track} distribution, the data sample is fitted with three templates, as shown in figure 6, a $\tau_{\mathrm{had-vis}}$ and electron template (real electrons from $t\bar{t}$ events, either prompt or from leptonic τ decays, contribute significantly to the signal region); a gluon-jets template (fake $\tau_{\mathrm{had-vis}}$ candidates from QCD multijets); and a quark-jets template (fake $\tau_{\mathrm{had-vis}}$ from $t\bar{t}$). Finally, fraction of $\tau_{\mathrm{had-vis}}$ candidates from fitted $\tau_{\mathrm{had-vis}}$ and electron template is obtained using Monte Carlo simulation. The resulting cross section is $200 \pm 19(\mathrm{stat}) \pm 43(\mathrm{syst})$ pb. The measured cross section is consistent with the theoretical prediction, 164^{+11}_{-16} pb. Dominant systematics for the analysis are initial and final state radiation and b-jet tagging uncertainties.

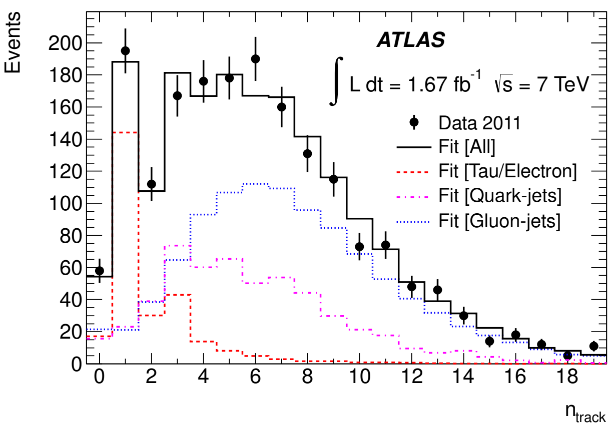

Fig. 6. The n_{track} distribution for $\tau_{\mathrm{had-vis}}$ candidates after all selection cuts. The black points correspond to data, while the solid black line is the result of the fit. The dashed, dotted and dash-dotted histograms show the fitted contributions from the $\tau_{\mathrm{had-vis}}$ signal, and the gluon-jet and quark-jet backgrounds, respectively [9].

6.2. τ+leptons final state

This analysis uses 2.05 fb^{-1} of data collected from proton–proton collisions at a centre-of-mass energy of 7 TeV. The final states with one light lepton (e/μ), one $\tau_{\mathrm{had-vis}}$ candidate, at least two jets and $E_{\mathrm{T}}^{\mathrm{miss}}$ are considered. Events are selected by a single lepton trigger. At least one of the jets is required to be identified as originating from a b-quark. The $\tau_{\mathrm{had-vis}}$ candidate is required to have 1 or 2, 3 tracks.

The dominant background comes from $t\bar{t} \to$ lepton + jets events where one jet is misidentified as $\tau_{\mathrm{had-vis}}$. Therefore, the τ identification (ID) is crucial to obtain a decent signal purity. Instead of requiring τ identification requirements, this analysis uses the score spectrum of the τ ID boosted decision tree (BDT) [3]. The number of τ leptons in a sample is extracted by fitting the distributions of BDT outputs to background and signal templates. The BDT output shape for the background is extracted from the zero b-jet control sample after subtracting real $\tau_{\mathrm{had-vis}}$ contributions using simulation. Background contributions with misidentified $\tau_{\mathrm{had-vis}}$ are estimated by exploiting the charge correlation between the lepton and the misidentified $\tau_{\mathrm{had-vis}}$ in QCD multijet events. Events, in which the $\tau_{\mathrm{had-vis}}$ has the same reconstructed charge (SS) as the lepton, are subtracted from the opposite sign (OS) sample leading to a cancellation of the QCD multijet background. The signal template is derived from τ candidates in the MC simulation that

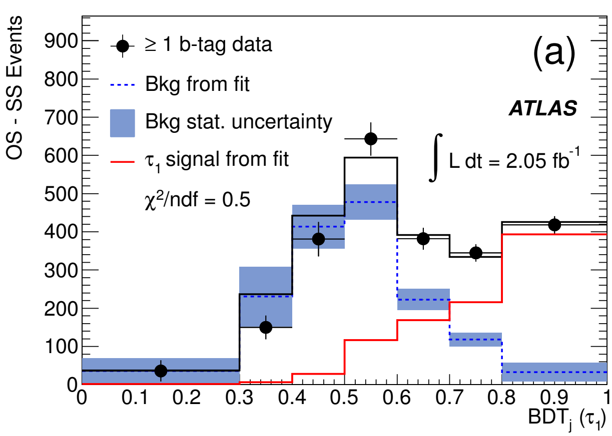

Fig. 7. BDT (OS-SS) distributions in events with lepton + 1-prong $\tau_{\mathrm{had-vis}}$ in the signal sample. The normalization of each template is derived from a fit to the data. The fitted contributions are shown as the light grey/red (signal), dashed/blue (background derived from 0 b-tag region after applying MC corrections) and black (total) lines. Shaded/blue bands are the statistical uncertainty of the background template [8].

are truth-matched to a real τ-lepton in the proportion expected from simulated events passing the event selection. $Z \to \tau\tau$ and diboson processes are also included as they include real τ leptons. Those contributions are subtracted from the number of signal events obtained from the fit, before calculating the cross section.

Figure 7 shows the BDT score distribution for real and misidentified $\tau_{\mathrm{had-vis}}$ candidates. The normalization of each template is derived from a fit to the data. The combined cross section for electron and muon final states and for 1-prong and 3-prong $\tau_{\mathrm{had-vis}}$ candidates is $186 \pm 13(\mathrm{stat}) \pm 20(\mathrm{syst})$ ± 7 (lumi) pb, which is consistent with the theoretical prediction, 164^{+11}_{-16} pb.

The main systematics arise from efficiency of the b-tagging algorithm, initial and final state radiation uncertainty and τ identification.

7. Measurement of τ polarization

Another very interesting study involving τ leptons is the measurement of τ polarization in $W \to \tau\nu$ decays [10]. This is the first measurement of τ polarization at a hadron collider.

Given the short lifetime and their maximal parity violating decays, τ leptons are the only leptons whose spin information is reconstructable from the decay products recorded in ATLAS. The τ polarization, P_τ, is defined as the asymmetry between the left-handed and right-handed τ production cross sections of a given process. In $W \to \tau\nu$ decays, the SM predicts a polarization of -1, reflecting the parity violating structure of the charged weak current. Parity conserving interactions like a $H \to \tau\tau$ decay would yield to $P_\tau = 0$. On the other hand, a supersymmetric charged scalar Higgs boson decaying via $H^+ \to \tau\nu$ is expected to produce $P_\tau = +1$. Tau polarization may, therefore, be used as a discriminating variable in searches for this particle.

The dominant 1-prong hadronic τ decay mode is $\tau^- \to \rho^-\nu \to \pi^-\pi^0\nu$ (BR $\sim 25\%$). In this decay channel, the spin information of the τ is transferred to the intermediate ρ meson due to the maximal parity violating charged current. Angular momentum conservation results in a preference of left-handed τ leptons to decay to a transversely polarized ρ, leading to a symmetric energy sharing between the two pions in the final state. A longitudinal ρ polarization would be preferred in hypothetical non-SM decays to right-handed τ leptons, leading to an asymmetric energy sharing. An observable constructed to be sensitive to the energy sharing between charged ($E_{\mathrm{T}}^{\pi^-}$) and neutral ($E_{\mathrm{T}}^{\pi^0}$) pion, and therefore the polarization Υ, is defined as

$$\Upsilon = \frac{E_{\mathrm{T}}^{\pi^-} - E_{\mathrm{T}}^{\pi^0}}{p_{\mathrm{T}}}\,, \tag{2}$$

where $p_{\rm T}$ is a $\tau_{\rm had-vis}$ candidate transverse momentum. Experimentally, the energy associated with the charged pion is given by the transverse momentum of the single track associated with the $\tau_{\rm had-vis}$ candidate. The energy of the neutral pion(s) is calculated as the difference between the $\tau_{\rm had-vis}$ transverse momentum (measured in the calorimeter) and the track transverse momentum of the $\tau_{\rm had-vis}$ candidate, $p_{\rm T}^{\rm trk}$. Thus $\Upsilon \sim 2p_{\rm T}^{\rm trk}/p_{\rm T} - 1$.

The data, corresponding to an integrated luminosity of 24 pb^{-1} at $\sqrt{s} = 7$ TeV is selected with a combined trigger based on the presence of a $\tau_{\rm had-vis}$ candidate and $E_{\rm T}^{\rm miss}$. Events are required to fulfill certain criteria to select $W \to \tau\nu$, similar to these described in Section 4. After passing identification criteria, the $\tau_{\rm had-vis}$ candidate is in addition required to have a single associated track to enrich the sample in $\tau^- \to \pi^-\pi^0$ decays.

Two distinct simulated $W \to \tau\nu$ signal samples are generated forcing the τ lepton to decay as a left- or right-handed τ, respectively. The polarization P_τ is extracted by a binned likelihood fit of the data to a parametrized template, obtained by linear interpolation between the two simulated extreme cases of $P_\tau = 1$ and $P_\tau = -1$. The result is shown in figure 8. The measured polarization is $P_\tau = -1.06 \pm 0.04(\mathrm{stat})^{+0.05}_{-0.07}(\mathrm{syst})$ and well in agreement with the SM expectation of $P_\tau = -1$.

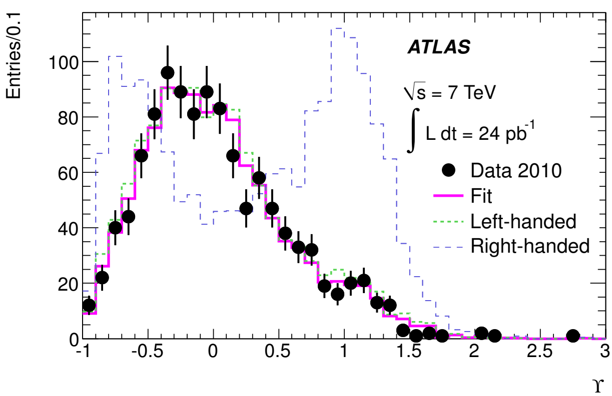

Fig. 8. Simulated signal and background templates for left-handed and right-handed τ decays along with the observed charged asymmetry distribution in data. The best fit resulting from maximizing the likelihood is plotted in bold [10].

8. Summary

ATLAS has a very rich programme in τ physics, which include both Standard Model and New Physics measurements. The τ reconstruction and identification algorithms used by the experiment have proven to be effective at providing discrimination against QCD jets and electrons in such measurements, which is crucial to establish the presence of τ leptons in any event. These algorithms are fully commissioned and validated in data.

One of the first tests of a robust τ lepton identification and reconstruction was the cross section measurements of the W and Z bosons decaying to τ leptons and later of $t\bar{t}$ processes with τ leptons in final state. All measured cross sections are in good agreement with the SM predictions.

Also the first measurement of τ polarization at hadron collider has been performed. The small statistical and systematic uncertainties of this measurement demonstrate the potential of this method.

REFERENCES

[1] ATLAS Collaboration, Expected Performance of the ATLAS Experiment: Detector, Trigger and Physics, CERN-OPEN-2008-020,2008.

[2] Particle Data Group, *J. Phys. G* **37**, 075021 (2010).

[3] ATLAS Collaboration, Performance of the Reconstruction and Identification of Hadronic tau Decays in ATLAS with 2011 Data, ATLAS-CONF-2012-142, 2012.

[4] ATLAS Collaboration, *JINST* **3**, S08003 (2008).

[5] ATLAS Collaboration, $Z \to$ tau tau Cross Section Measurement in Proton–Proton Collisions at 7 TeV with the ATLAS Experiment, ATLAS-CONF-2012-006, 2012.

[6] S. Catani *et al.*, *Phys. Rev. Lett.* **103**, 082001 (2009).

[7] ATLAS Collaboration, *Phys. Lett.* **B706**, 276 (2012).

[8] ATLAS Collaboration, *Phys. Lett.* **B717**, 89 (2012).

[9] ATLAS Collaboration, *Eur. Phys. J.* **C73**, 2328 (2013).

[10] ATLAS Collaboration, *Eur. Phys. J.* **C72**, 2062 (2012).